Numerical simulation and experimental investigation of heat transfer and flow structures around heated spherical bluff bodies

Numerical simulation and experimental investigation of heat transfer and flow structures around heated spherical bluff bodies

A H Abed[1, 2], S E Shcheklein[1], V M Pakhaluev[1]

[1]Ural Federal University named after the first President of Russia B. N. Yeltsin
19 Mira St., Yekaterinburg 620002, Russia
[2]University of Technology, Al-Sinaa' Street, 10066, Baghdad, Iraq

E-mail: akraaam82@yahoo.com

Abstract. The objective of this work is to evaluate the influence of vortices on heat transfer behaviour and a flow structure around a heated sphere. Numerical simulation and experimental verification are performed using a stationary copper sphere located inside a cylindrical channel with a constant channel-to-sphere diameter ratio. Numerical simulation is done for three-dimensional steady-state flow using ANSYS-FLUENT by solving the Reynolds-averaged Navier Stokes (RANS) equations. Over the test range of Reynolds numbers (2500-55000), CFD simulation results are in reasonable agreement with experimental data. The importance of vortices on heat transfer behaviour was investigated by taking the surface temperature and heat transfer coefficient (HTC) measurements around the sphere surface as a function of a zenith angle. The CFD simulation results confirmed that the impact of vortices on heat transfer behavior occurred in a lower-rear area of the sphere with a zenith angle (from 120° to 180°).

1. Introduction

The heat transfer and flow characteristics around heated spherical bluff bodies are one of actively and widely researched problems due to their notable importance in many engineering applications such as nuclear power plants, food and chemical processing, towed sonar system and so on. The wake flow structure of a sphere including the velocity profile, flow separation, vortex shedding, left and drag coefficients has been extensively, numerically and experimentally investigated. Tsutsui and Okamoto [1,2] experimentally investigated the flow characteristics and the aerodynamic forces over a sphere located inside a wind tunnel under varying sphere heights above a turbulent boundary layer and noted the wake flow pattern around a sphere. A number of investigations analyzed the flow pattern and the aerodynamic forces in a uniform flow. Ozgoren M et al. [3] carried out an experimental study of flow patterns in both the sphere and circular cylinders inserted in a free-stream flow at Re =5000-10000, respectively, using a flow visualization methods. Hassanzadeh et al. [4] numerically investigated the flow configuration around a sphere as well as location of the stagnation-point and size of the wake length for Re = 5000. They noted that at a small-gap ratio, the flow pattern becomes symmetric and the re-attachment point of flow occurs earlier. Abed et al. [5] experimentally studied the flow-patterns and drag force over a sphere immersed inside a cylindrical channel using particle image velocimetry (PIV) method and then applied a flow control at Re range (25-200). In the heat transfer field, the convective heat transfer downstream of bluff bodies depends on the many complex factors such as trailing vortices

and the flow pattern interactions with the thermal boundary layer. Fisher and Sabatino [6, 7] experimentally investigated the vortices influence on heat transfer rate of a flat plate using circular cylinder and a tapered cylinder. They pointed out that the region of heat transfer enhancement has achieved near the center-line downstream with Stanton numbers range from 10 to 50. Furthermore, Vortex shedding forces and velocity profile changing downstream of a spherical bluff body leads to a vibration load and an additional unsteady lift and drag forces that leads to intensifying structural damage and sphere instability especially in high critical Re number. To avoid such damage, the weak flow pattern should be analyzed and investigated as well in high critical Re number. In this sense, this work aims to numerically investigate by the CFD method the heat transfer performance, boundary layer development and flow patterns of a stationary spherical bluff body located inside the cylindrical channel with a constant channel-to-sphere diameter ratio. The effects of the vortices on heat transfer and flow patterns downstream of the sphere are examined. In order to validate the CFD simulation method, the CFD results were compared with those obtained by experimental investigation.

2. Physical model and computational methods

A stationary sphere located inside the vertical cylindrical channel with the constant channel-to-sphere diameter ratio is considered here. Figure 1 depicts the schematic of the computational domain and boundary conditions in the present study. The computational domain consists of fluid entering the section, sphere section, and the outlet section. The diameters of the cylindrical channel and sphere are D and d, respectively and channel-to-sphere diameter ratio D/d was considered to be 1.35. For CFD simulation, some boundary conditions values were required such as the input heat flux, inlet air velocity, inlet air temperature, and so on. An inlet axial velocity of 0.89 – 18.9 m/s, inlet temperature of 298 K, and a wall heat flux of 10 kW/m^2 were adopted as boundary conditions in the present simulation study.

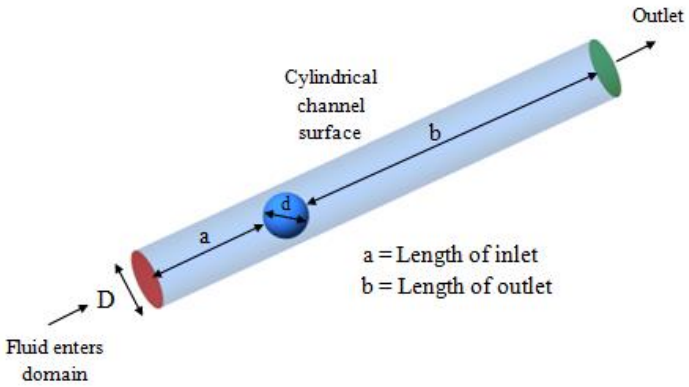

Figure 1. Schematic view of the geometrical for CFD simulations.

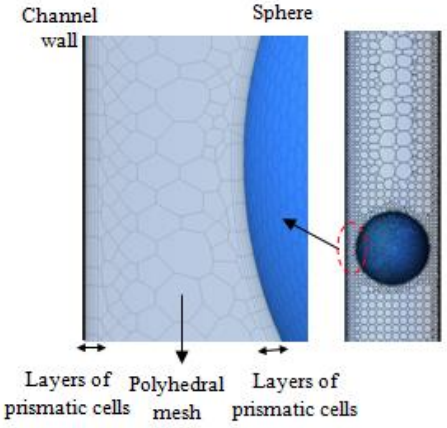

Figure 2. Meshes for the solid and in a region between a sphere and the wall channel

The ICEM CFD mesh generator was used to build the fine tetrahedral meshing elements with a number of prism cells layers near the boundary surfaces for better modeling of the flow field near the surface. Next, the TET mesh was converting to the polyhedral mesh in ANSYS Fluent as shown in figure 2. The major advantage of POLYs is that each individual element has many neighbors and is less sensitive to stretching, so the gradients of flow distribution can be much better than those having tetrahedral elements. This resulted in better numerical stability of the model [8]. In this work, the working fluid was defined to be incompressible, in which the density is considered to be constant with change in pressure over the sphere layer. The CFD simulations were performed using the commercial software ANSYS FLUENT v.17. Three dimensional Reynolds-averaged Navier–Stokes equations were employed for the simulation. Both laminar and turbulent flow regimes were carried out, the Re number was in the range $2500 < Re < 55000$. Laminar flow simulation was performed for Reynolds number

(Re = 2500) and the turbulent simulations for Reynolds numbers range 10000 < Re < 55000. The SST k-ω turbulence model which blended the advantages of the k-ε and k-ω models were applied in this simulation to obtain an optimal model formulation that accurately predicts the turbulent effect near the surface and improve the surface shear stress and heat transfer predictions. The modeled equations for the SST k-ω model can be written as:

Kinematic Viscosity

$$\nu_k = \frac{a_1 \kappa}{\max\left(a_1 \omega, SF_2\right)} \tag{1}$$

Turbulence Kinetic Energy

$$\frac{\partial \kappa}{\partial t} + U_j \frac{\partial \kappa}{\partial x_j} = P_\kappa - \beta^* \kappa\omega + \frac{\partial}{\partial x_j}\left[\left(\nu + \sigma_k \nu_k\right) \cdot \frac{\partial \kappa}{\partial x_j}\right] \tag{2}$$

Specific turbulence dissipation rate

$$\frac{\partial \omega}{\partial t} + U_j^{\cdot} \frac{\partial \omega}{\partial x_j} = \alpha S^2 - \beta\omega^2 + \frac{\partial}{\partial x_j}\left[\left(\nu + \sigma_\omega \nu_k\right)\frac{\partial \omega}{\partial x_j}\right] + 2\left(1 - F_1\right)\sigma\omega^2 \frac{1}{\omega}\frac{\partial \kappa}{\partial xi}\frac{\partial \omega}{\partial xi} \tag{3}$$

3. Experimental Setup and Procedure

In our study, the experimental setup was used to validate the CFD simulation and the reliability of simulation results. The experimental setup consists of an adiabatic boundaries cylindrical channel with a circular cross-section of the 50 mm outer diameter and the 2 mm wall thickness was set vertically. The test object was a copper sphere of the 34 mm diameter has independently heated using the 100W - electrical heater. Vaccum air blower was utilized and compact pitot-tube was installed to obtained the air velocity. Two calibrated (k-type) thermocouples were used to directly measure the mean average surface temperature. Further, the inlet and outlet air temperatures were recorded using two thermocouples placed immediately upstream and downstream of the cylindrical channel, respectively. Manometric fluid with a specific density of 0.95 was used in the inclined manometer to measurement of the pressure distribution across the sphere at a range of Re numbers. For each experiments, the surface temperature, air flow rate, inlet and outlet air temperatures and pressure drop were record under steady-state operating conditions in which the inlet air temperature kept constant at 24 °C. The temperature recorder, all thermocouples, and pitot-tube were calibrated prior to the experiment. Experiments were performed for a range of Reynolds number regimes (2500 - 55000) and a packing ratio of 1,35 of the channel-to-sphere diameter.

4. Results and discussion

In order to validate the reliability of the CFD simulation, CFD results were compared with those obtained from related experimental measurements. The comparison between CFD simulation and experiment of average surface temperature and heat transfer coefficient for a range of Re numbers are depicted in figures 2 and 3. It can be noticed that the heat transfer coefficient tends to increase with increasing of Re due to the increasing contribution from the convection and decreasing boundary-layer thickness. Over the test range of Reynolds numbers, CFD results are in reasonable agreement with experimental data.

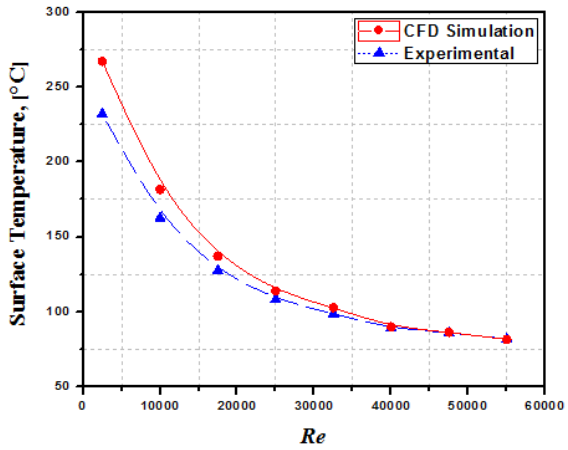

Figure 3. Comparison of average surface temperature.

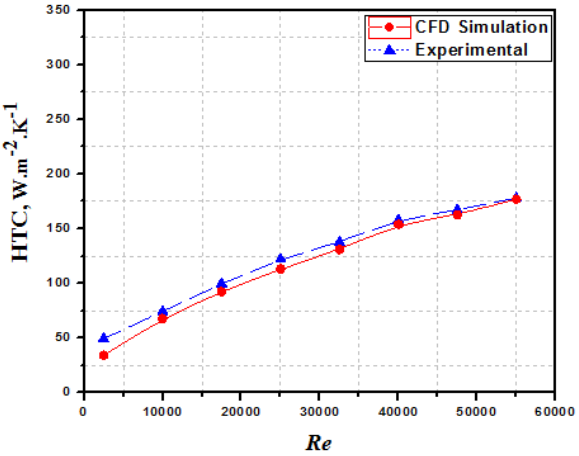

Figure 4. Comparison of heat transfer coefficient.

Figure 5 depicts the predicted temperature contours on the full sphere's surface. The color-index illustrates the magnitude of surface temperature. It is observed in this figure that lower surface temperature is indicated on the front of the sphere due to the impinging of airflow over the front region caused better heat transfer and higher surface temperature is obtained on the part of the rear region for the sake of flow separation. The distribution of the local temperature profile and the heat transfer coefficient over the sphere surface as a function of the azimuth angle [θ] calculated from the front stagnation point is shown in figures 6, 7. The maximum of surface temperature occurred around the angle of 110◦ as is obviously shown in Fig.6.

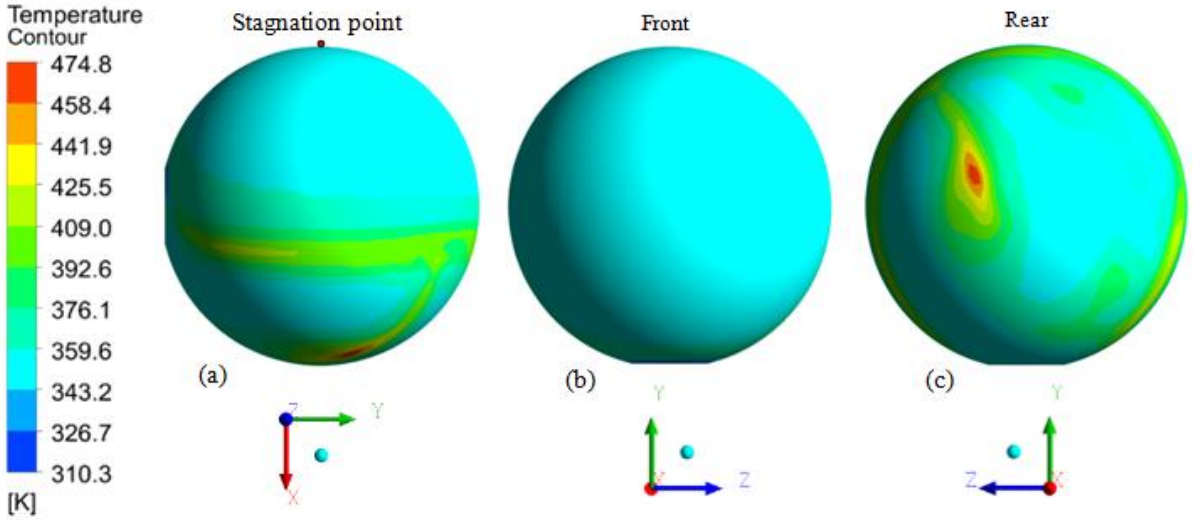

Figure 5. Temperature contours of a sphere: (a) side view, (b) front view, (c) rear view.

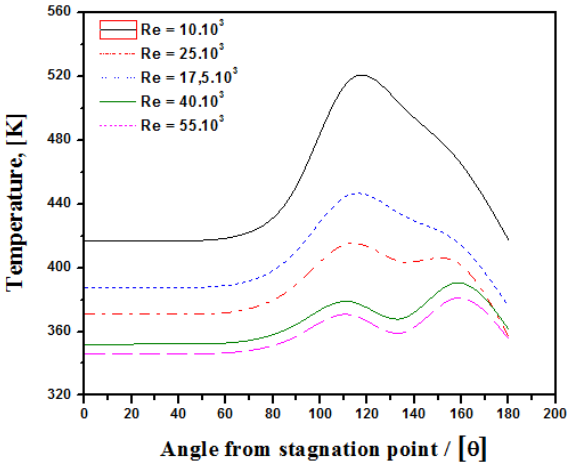

Figure 6. Local temperature profile as function of zenith angle calculated from stagnation-point

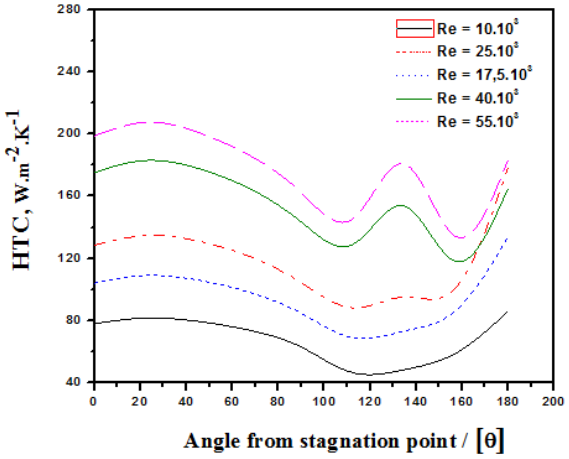

Figure 7. Local heat transfer coefficient as function of zenith angle calculated from stagnation-point

From figure 7 it can be noticed that the heat transfer coefficient (HTC) diminishment around the surface of the sphere with increasing the zenith angle (Up to 100°), then it significantly increases (from 120° to 180°). The region of increased heat transfer rate could be correlating with the generated vortices, fluctuating velocity and flow recirculation as they sweep air toward the surface as clearly shown in figure 8 The instantaneous velocity vector maps with CFD simulation is shown in figure 8. This figure gives a better understanding of flow patterns and the weak structure around the sphere in the effect of cylindrical channel boundary layer flow. The low channel-to-sphere diameter ratio has a significant effect on the wake structure due to the interaction between the velocity profile and sphere wake. With Re = 2500 it can be noted that the vortex patterns formed a symmetrically flow structure in the near sphere wake zone under the effect of the interaction due to the vortices of each individual sphere side.

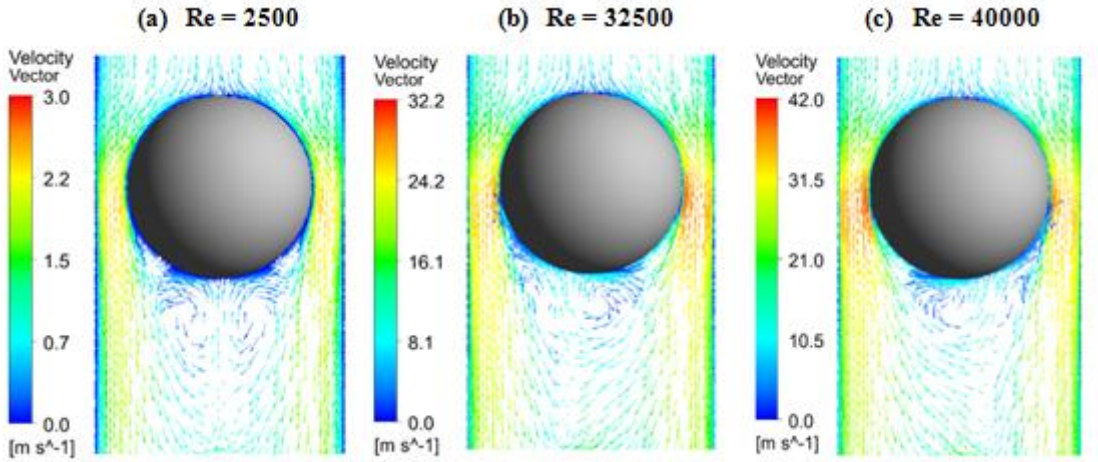

Figure 8. Velocity vector maps around sphere: (a) Re=2500, (b) Re=32500, (c) Re=40000.

As flow velocity increased (Re>2500), on each side of the sphere we developed lift forces leading to motion transverse to the flow, and vortices are not symmetrical. The pressure coefficient distributions around the sphere surface from the front stagnation point are shown in figure 9. The pressure coefficient on the front and rear regions of the sphere was positive, excepting the forward-lower region with the zenith angle between (75° to 120°) was found to be negative.

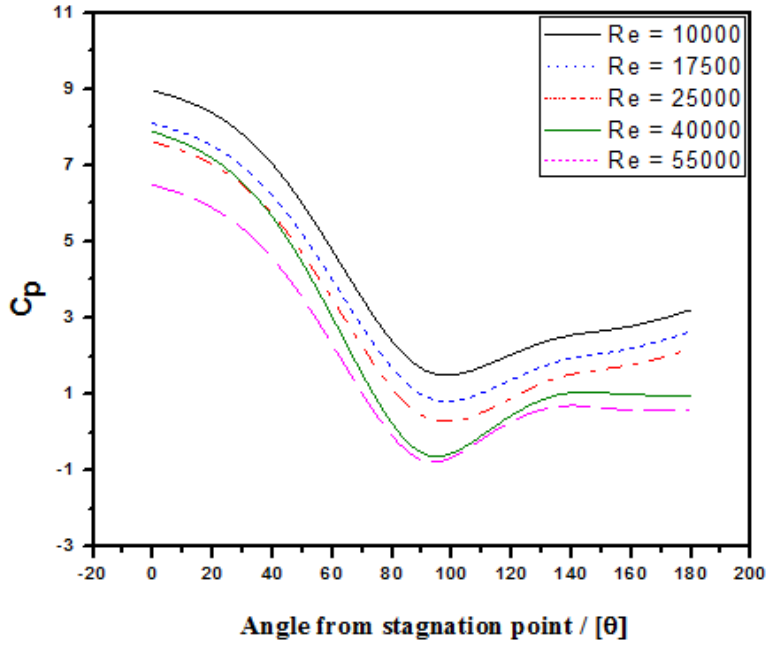

Figure 9. Pressure distribution as function of zenith angle calculated from stagnation-point

5. Conclusions

Heat transfer and flow characteristics around a heated sphere were studied numerically and experimentally in this paper. Impact of vortices on the heat transfer behaviour was studied under a range of Re numbers and the constant wall heat flux condition. The surface temperature profile was noted to be lower on the front of the sphere due to the impinging of air flow, and higher surface temperature was obtained on the part of the rear region for the sake of flow separation. In a lower-rear area of the sphere (from 120° to 180°) the impact of vortices on the heat transfer behaviour occurred, and enhanced heat transfer was achieved.

References

[1] Tsutsui T 2008 *J. Wind Eng. Ind.* **96** 779–792.
[2] Okamoto S 1980 *Turbulent Shear Flow* **2** 246–256.
[3] Ozgoren M, Pinar E, Sahin B and Akilli H 2011 *International Journal of Heat Fluid Flow* **32 (6)** 1138-1146.
[4] Hassanzadeh R, Sahin B and Ozgoren M 2011 *International Journal of Computational Fluid Dynamics* 25 (10) 535–545.
[5] Abed A and Shcheklein, S 2018 *Journal of Physics: Conference Series* **1015** 032001.
[6] Fisher E M and Eibeck PA 1990 *Journal of heat transfer* **112(2)** 329-335.
[7] Sabatino D R and Smith C R 2009 *Journal of Turbomachinery* **131(1)** 011015.
[8] Sosnowski M, Krzywanski J and Gnatowska R 2017 *E3S Web of Conferences* **14** 01027